Direct Observation of Giant Pickering Emulsion and Colloidosome Droplet Interaction and Stability

ARTICLE *in* LANGMUIR · OCTOBER 2012

Impact Factor: 4.46 · DOI: 10.1021/la3025765 · Source: PubMed

6 AUTHORS, INCLUDING:

Kate L Thompson
The University of Sheffield
25 PUBLICATIONS **455** CITATIONS
SEE PROFILE

Grant B Webber
University of Newcastle
48 PUBLICATIONS **781** CITATIONS
SEE PROFILE

Steven P Armes
The University of Sheffield
612 PUBLICATIONS **27,677** CITATIONS
SEE PROFILE

Erica J Wanless
University of Newcastle
81 PUBLICATIONS **2,511** CITATIONS
SEE PROFILE

Langmuir

Article

pubs.acs.org/Langmuir

Direct Observation of Giant Pickering Emulsion and Colloidosome Droplet Interaction and Stability

Kate L. Thompson,[†] Emma C. Giakoumatos,[‡] Seher Ata,[‡,§] Grant B. Webber,[‡] Steven P. Armes,[†] and Erica J. Wanless*[,‡]

[†]Department of Chemistry, University of Sheffield, Brook Hill, Sheffield, South Yorkshire, S3 7HF, United Kingdom

[‡]Priority Research Centre for Advanced Particle Processing and Transport, University of Newcastle, Callaghan, NSW, 2308, Australia

[§]School of Mining Engineering, University of New South Wales, Sydney, NSW 2052, Australia

Supporting Information

ABSTRACT: The interactions of two 2-mm pendant oil droplets grown in the presence of an aqueous solution of poly(glycerol monomethacrylate)-stabilized polystyrene latex particles was observed using a high-speed video camera. The coalescence behavior was monitored as a function of oil type (*n*-dodecane versus sunflower oil) and particle size (135 versus 902 nm), as well as in the presence and absence of an oil-soluble cross-linker [tolylene 2,4-diisocyanate-terminated poly(propylene glycol)]. The damping coefficient of the coalescing *n*-dodecane droplets was found to increase in the presence of the latex, demonstrating particle adsorption. Coalescence times increased when the oil phase was changed from *n*-dodecane to sunflower oil, because of the much higher viscosity of the latter oil. In addition, increasing the adsorbed particle size from 135 to 902 nm led to longer coalescence times because of the greater distance separating the oil droplets. Coalescence times observed in the presence of the larger 902-nm particles indicated that two different modes of contact can occur prior to a coalescence event (bilayer or bridging monolayer of particles in the film). Addition of an oil-soluble surface-active cross-linker to the sunflower oil phase to react with the hydroxy groups of the particle stabilizer reduced the interfacial elasticity and ultimately prevented coalescence after cross-linking for 20 min at 25 °C. Such giant colloidosomes can remain in contact for several hours without undergoing coalescence, which demonstrates their high stability. Furthermore, coalescence is prevented even if the cross-linker is present in only one of the pendant droplets. Finally, evidence for cross-linker diffusion from one pendant droplet to another was indicated by a visible filament connecting the two droplets upon retraction.

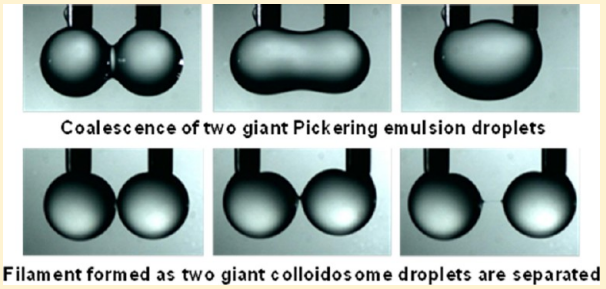

INTRODUCTION

The stabilization of oil and water droplets by solid particles has been known for over a century, and these formulations are generally referred to as Pickering emulsions.[1] Stabilization of such emulsions occurs when the particles are wetted by both the aqueous and oil phases. Wettability is determined by the three-phase contact angle (θ) that the particle makes with the oil/water interface. Hydrophilic particles have contact angles of less than 90° and stabilize oil-in-water (o/w) emulsions, whereas more hydrophobic particles display contact angles of greater than 90° and stabilize water-in-oil (w/o) emulsions.[2] Silica,[3] clays,[4] and polymer latex particles[5,6] have all been used successfully as Pickering emulsifiers. Stimulus-responsive Pickering emulsifiers have also been investigated, with demulsification or phase inversion being achieved in response to changes in solution temperature[7] or pH.[6,8]

The long-term stability of Pickering emulsions is attributed to the relatively high interfacial detachment energies of the adsorbed particles at the oil/water interface.[2] This prevents particle desorption during thin-film drainage and provides a steric barrier to coalescence with neighboring droplets.[9,10] The stability of the intervening thin film depends strongly on the size, shape, contact angle, and concentration of particles at the interface. For Pickering emulsions stabilized by spherical polymer latexes, hexagonal-close-packed monolayers of adsorbed particles have been confirmed using critical-point drying and scanning electron microscopy.[11] This indicates that neighboring droplets interact across a film bounded by impinging bilayers of adsorbed particles. The resulting emulsion droplet diameter increases with increasing particle size[12] with larger particles generally being more strongly adsorbed at the oil/water interface than smaller ones.[2]

In recent years, Pickering emulsions have been used as a template for the preparation of microcapsules. Such microcapsules are known as colloidosomes[13] and can be prepared using various techniques. Neighboring particles can be locked together by methods including thermal annealing,[13−15] gel trapping,[16,17] polyelectrolyte complexation,[18−20] and covalent

Received: June 26, 2012
Revised: September 18, 2012
Published: October 22, 2012

cross-linking.[21−25] The first examples of such structures were reported by Velev and co-workers.[26−28] Latexes were assembled at the water/*n*-octanol interface and then locked in place by the addition of a strong coagulant (casein, HCl, and $CaCl_2$). Dinsmore et al.[13] prepared colloidosomes by thermal annealing, whereby they heated the Pickering emulsions to above the glass transition temperature of the polystyrene latex forming the shell. Ashby et al.[29] prepared giant pendant colloidosomes by assembling polystyrene latexes at the oil/water interface. An aqueous solution of polystyrene particles was suspended from a capillary into the oil phase. This particle-stabilized droplet was then carefully transferred through a planar oil/water interface to form a pendant water−oil−water colloidosome. No sintering or cross-linking step was required in this case, as the particles were supported by an oil film bridging the latex monolayer. Recently, Thompson et al. prepared a series of poly(glycerol monomethacrylate)-stabilized polystyrene (PGMA−PS) latexes that acted as efficient o/w Pickering emulsifiers for a range of model oils.[24,25,30] Latexes were cross-linked with their neighbors from the internal oil phase using a polymeric diisocyanate cross-linker. Such covalently cross-linked colloidosomes were sufficiently robust to survive the removal of the internal oil phase by washing with excess ethanol.

Ata has reported a powerful direct method for investigating bubble or droplet coalescence using a high-speed video camera.[31] As a model for froth flotation, glass beads with a mean diameter of 66 μm were adsorbed onto ∼2 mm diameter air bubbles, and average coalescence times were recorded at up to 3700 frames/s. Analysis of the coalescing bubble projected area revealed damped simple harmonic motion for particle-coated bubbles compared to particle-free bubbles. Particle hydrophobicity was demonstrated to play an important role, with adsorbed surfactant used to increase contact angle and thus reduce bead detachment upon coalescence. The coalescence of air bubbles stabilized by submicrometer-sized poly(ethylene glycol) methacrylate- (PEGMA-) stabilized poly(2-vinylpyridine) latexes has also been investigated using this apparatus.[32] These cationic particles are highly effective for stabilizing foams, but catastrophic foam collapse occurs when the particles undergo an acid-induced latex-to-microgel transition.[33] This transition was evident in the rapid coalescence and postrupture dynamics observed for two air bubbles prepared in the presence of these particles. Recently, this high-speed video apparatus was also successfully deployed to investigate the coalescence of two kerosene droplets in aqueous solution as a model for kerosene emulsions.[34] Droplet coalescence times varied with both the droplet age and kerosene grade. The longer coalescence times were correlated with the more vigorous postrupture oscillations recorded during drop fusion. This reduction in the damping of the coalescing drop motion was attributed to an increase in interfacial elasticity. No added surfactant or particles were present during these experiments.

In the current work, we utilize high-speed video imaging to monitor the interactions of millimeter-sized oil droplets in water coated with an adsorbed monolayer of the previously reported sterically stabilized PGMA−PS latexes.[24,25,30] The effects of oil type and particle diameter on the coalescence time and postrupture oscillations of the coalescing droplet pairs are investigated. In addition, an oil-soluble polymeric cross-linker was dissolved in the oil phase to achieve covalent stabilization of the giant latex superstructure. The stability and coalescence behavior of such pendant colloidosomes were also investigated as a function of oil and particle size.

EXPERIMENTAL SECTION

Materials. *n*-Dodecane (>99% purity), sunflower oil, tolylene 2,4-diisocyanate-terminated poly(propylene glycol) (PPG-TDI; 97% purity), and potassium chloride (>99% purity) were all purchased from Aldrich and used as received. Millipore Milli-Q water was used in all experiments.

$PGMA_{50}$−PS Latex Synthesis. $PGMA_{50}$−PS latexes of 135- and 902-nm diameter were prepared using a $PGMA_{50}$ macromonomer by either aqueous emulsion or alcoholic dispersion polymerization. Full details of the macromonomer and latex syntheses have been reported previously.[30] The particles were purified by repeated centrifugation into pure water. This cleanup protocol led to aqueous dispersions of 6.42 and 5.27 wt % for the 135- and 902-nm particles, respectively.

Transmission Electron Microscopy (TEM). TEM (Phillips CM100 instrument operating at 100 kV) studies were conducted on samples prepared by drying a drop of dilute aqueous dispersion on a carbon-coated copper grid.

Scanning Electron Microscopy (SEM). SEM studies were performed using an FEI Sirion field-emission scanning electron microscope with a beam current of 244 μA and a typical operating voltage of 20 kV. Samples were dried onto aluminum stubs and sputter-coated with a thin layer of gold prior to examination so as to prevent sample charging.

Droplet Coalescence Apparatus. The apparatus used in this work was reported previously for studying the coalescence of two air bubbles[31,32] or kerosene droplets[34] in aqueous solution. Two stainless steel capillaries (0.41-mm inner diameter and 0.71-mm outer diameter) were inserted into a beaker containing 50 mL of an aqueous latex dispersion and a magnetic stirrer bar. Two microsyringe pumps (Sarasota, FL) were used to produce either sunflower oil or *n*-dodecane oil droplets from the tips of the capillaries. During all experiments, the stirrer speed was set at 100 rpm, which was slow enough to avoid detachment of the oil droplets from the capillaries. Between experiments, the glassware, syringes, capillaries, and stirrer bar were thoroughly cleaned using 2-propanol to remove any oil residue and then rinsed with Millipore Milli-Q water at least 10 times to remove any residual contaminants.

Coalescence data were recorded using a high-speed video camera (Phantom 4, vision research) at a rate of up to 2100 frames/s. Images were collected using Phantom 6.30 (Nikon) software at 512 × 256 resolution. A light source was used for back illumination of the droplets.

Sample Preparation. The particle suspensions used in this work were required to be of sufficiently low turbidity to enable high-quality high-speed video capture. For solutions of the larger 902-nm latex, 5 μL of a 5.27 wt % dispersion was added to the beaker (4-cm diameter) containing 50 mL of water. This led to a latex concentration of 5.3×10^{-4} wt %. It was not possible to work with significantly higher concentrations of this larger latex, as these dispersions became too turbid for the pendant oil droplets to be clearly observed. Two concentrations of the 135-nm $PGMA_{50}$−PS particles were investigated. Either 23 μL of a 0.17 wt % dispersion or 15 μL of a 6.42 wt % dispersion of latex was added to 50 mL of water. This led to latex concentrations of 7.8×10^{-5} or 1.9×10^{-3} wt %, respectively. The latter was used for most of the experiments.

Droplet Coalescence Procedure and Data Analysis. The oil of interest was held in the two syringes and then connected to the capillaries; care was taken to avoid any trapped air bubbles in the syringes. The beaker was filled with 50 ± 1 mL of water to which a predetermined amount of concentrated aqueous latex dispersion was added by a micropipet (see earlier). This sample beaker was then placed inside a rectangular Perspex vessel containing water to prevent optical distortion arising from the cylindrical surface of the beaker. Approximately 2 mL of oil was carefully pipetted onto the top of the aqueous dispersion in the beaker. This was required to saturate the aqueous phase with oil, to maintain a constant oil/aqueous dispersion

dx.doi.org/10.1021/la3025765 | *Langmuir* 2012, 28, 16501−16511

interfacial area throughout the experiments, and to minimize evaporation effects. The vessel containing the beaker was then placed on top of a magnetic stirrer mounted on a laboratory jack beneath the capillaries. The two capillaries could then be immersed in the aqueous dispersion in the beaker. The capillaries were adjusted to a standard separating gap of ~1.8 mm, and the syringe pump rate was set at 0.3 mL/h. The two microsyringe pumps were then started to release the oil from the tips of the capillaries. Once the droplets reached ~2.0 mm in diameter, the microsyringe pumps were stopped. At this point, the latex dispersion was stirred at 100 rpm, and a stop watch was used to determine the length of time for which the droplets were exposed to the aqueous phase (termed the droplet aging time). After a predetermined aging time, the stirrer was stopped, and the capillaries were moved together using a linear actuator at a speed of 0.238 cm/s until the droplets were just touching (capillary separation of ~1.2 mm). The droplet coalescence time was measured from the point of droplet first contact until coalescence and was analyzed from the video footage at 40−300 frames/s. Each experiment was repeated at least 15 times, and the mean and standard deviation of the coalescence time were recorded.

Another series of videos was recorded to capture the dynamic oscillations that occurred after droplet coalescence.[32,34] These videos were recorded at a resolution of 512 × 256 using a frame rate of 2100 frames/s to allow for detailed analysis of the postcoalescence behavior. The projected surface area of the droplets before, during, and after coalescence was measured as a function of time. The droplet area in each frame of video was analyzed using Image J software, and the results were plotted as the percentage change in the projected droplet area relative to the initial area of droplets observed immediately prior to coalescence.

Cross-Linking Experiments. For the cross-linking experiments, the same protocol as described above was followed. The pure oil phase in the syringes was replaced with a solution of PPG-TDI cross-linker in the appropriate oil at a concentration of 1 mg/mL.[24]

Pendant Drop Tensiometry. Interfacial tension measurements of single pendant oil drops (10 μL) suspended in water and aqueous latex dispersions were measured using a PAT-1 tensiometer (SINTERFACE Technologies, Berlin, Germany). The interfaces of sunflower oil and *n*-dodecane droplets with the aqueous solution were investigated in both the presence and absence of 1 mg/mL PPG-TDI dissolved in the oil phase. These particle-free interfaces were then compared to pendant sunflower oil drops in contact with an aqueous phase containing 1.3×10^{-3} wt % of the 135-nm diameter latex. Following a period of equilibration, each pendant drop was subjected to a ±1 μL volume oscillation with a period of 5 s for 10 complete cycles in order to assess the impact of the adsorbed latexes on the interfacial viscosity and elasticity. The data presented are the means and standard deviations of between two and eight runs.

Bulk Viscosity Measurements. The viscosity of the sunflower oil and *n*-dodecane with and without 1 mg/mL PPG-TDI cross-linker was measured using a TA Instruments AR-G2 controlled-stress rheometer. The viscosities were found to be 52 mPa·s for sunflower oil and 1.36 mPa·s for *n*-dodecane, in both the presence and absence of 1 mg/mL PPG-TDI. Therefore, addition of the cross-linker has no detectable effect on the bulk viscosity of the two oils used in this study.

RESULTS AND DISCUSSION

Bare Oil Droplet Interactions. Initially, the behavior of the pure-oil interfaces was investigated. The equilibrium interfacial tensions for the pure *n*-dodecane/water and sunflower oil/water interfaces are summarized in Table 1. The interfacial tension of the sunflower oil/water interface was approximately half that of the *n*-dodecane/water interface. In addition, the interfacial tension of each oil containing PPG-TDI was measured against water. PPG-TDI can be considered highly surface active, as it lowers the interfacial tension significantly for both oils; see Table 1.

Table 1. Equilibrium Interfacial Tension of the Various Oil/Aqueous Solution Interfaces Investigated

interface	equilibrium interfacial tension (mN/m)
n-dodecane/water	47.2 ± 2.9
(*n*-dodecane + PPG-TDI)/water	12.2 ± 0.4
sunflower oil/water	21.3 ± 1.6
(sunflower oil + PPG-TDI)/water	9.5 ± 0.2

Initial oil droplet coalescence studies were conducted in the absence of latex particles. Surprisingly, coalescence rarely occurred for both bare pure oil/water interfaces for a droplet aging time of 2 min. Such high stability for bare oil droplets appears at first glance to be counterintuitive, as stable emulsions are not usually achieved under such conditions. However, there is literature precedent for such stable pure-oil droplets. So-called "surfactant-free" emulsions of *n*-dodecane-in-water have been prepared in the absence of any stabilizer using a freeze−thaw technique.[35] The emulsion stabilization mechanism is believed to be due to a buildup of negative charge on the surface of the oil droplets due to adsorption or reaction of hydroxide ions.[36,37] The zeta potential of such bare *n*-dodecane droplets in water was measured to be −58 ± 7 mV.[38] This strong anionic charge leads to electrostatic repulsion between droplets, resulting in emulsion stability in the absence of any surface-active species. Tabor et al.[39] reported similar findings, with bare oil droplets failing to coalesce even when pushed together. In this case, coalescence could be induced by lowering the solution pH or by introducing electrolyte, either of which would reduce the effective surface charge on the oil droplets. In the present work, coalescence did occur for shorter droplet aging times (<1 min) or in the presence of electrolyte (0.1 M KCl). However, the minimum droplet aging time required to prevent coalescence is well in excess of the millisecond time scale of hydroxide ion adsorption,[40] and thus, it is likely that thermal fluctuations and movement of molecules at the freshly formed interface are contributing to the observed instability. Therefore, the stability of the 2-min-aged bare oil droplets is most likely due to the combined effects of electrostatic repulsion caused by the sufficient buildup of anionic surface charge and the attainment of a physical steady state with time.

For those events where the two oil droplets coalesced (i.e., for short aging times or in the presence of added electrolyte), the resulting single droplet was found to undergo dynamic oscillation until the energy was dissipated into the aqueous phase and an equilibrium state was achieved. Analysis of such oscillatory behavior was achieved by a frame-by-frame examination of the video footage, recording the change in projected surface area of the coalescing droplets with time (see Figure S1, Supporting Information). These oscillatory data were fitted to a damped simple harmonic oscillator with a damping coefficient.[41] The damping coefficients of the two oil droplet coalescence events were calculated to be 0.0331 and 0.0671 $m \cdot s^{-1}$ for the *n*-dodecane and sunflower oil interfaces, respectively. This difference in damping rates is attributed to the differing oil viscosities because the *n*-dodecane damping coefficient is similar to that of kerosene (0.0335 $m \cdot s^{-1}$ with 1.64 mPa·s viscosity) droplets reported previously.[34]

Pickering Droplet Interactions. After the pure-oil interfaces had been investigated, latex particles were added to the system. Transmission and scanning electron microscopy images of the two latexes used in this study are shown in Figure 1. Such latexes have previously been shown to be efficient

dx.doi.org/10.1021/la3025765 | Langmuir 2012, 28, 16501−16511

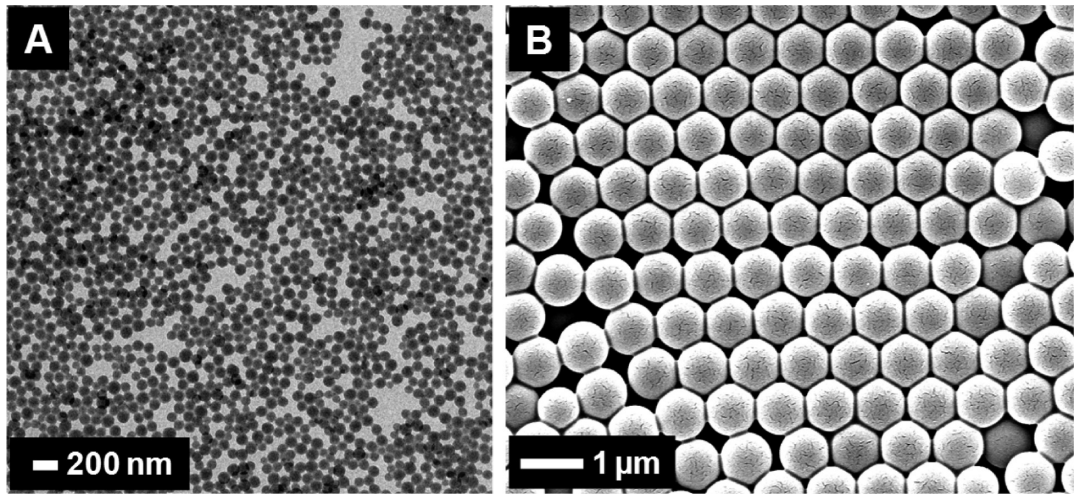

Figure 1. (A) Transmission electron microscopy image of 135-nm $PGMA_{50}$–PS latex particles prepared by aqueous emulsion. (B) Scanning electron microscopy image of 902-nm $PGMA_{50}$–PS latex particles prepared by alcoholic dispersion polymerization.

Pickering emulsifiers for both oils used in this study.[24,25] The resulting emulsions are highly stable, with no signs of any demulsification upon standing after many months. Previously, these $PGMA_{50}$–PS latexes were shown to adsorb as a close-packed monolayer at the oil/water interface with few or no particles remaining in the aqueous phase after homogenization, up to a certain critical latex concentration.[24] In addition, the contact angle for 600–1100-nm PGMA–PS latexes adsorbed at the *n*-dodecane/water interface was recently estimated to be 75° ± 6° using both a gel-trapping technique and the film calliper method.[42] That work also demonstrated that the measured contact angles were independent of particle size for the range investigated. The contact angle for the PGMA–PS latexes at the sunflower oil/water interface has not been measured, although it is anticipated to be similar to or perhaps slightly higher than that at the *n*-dodecane/water interface because of the polar triglyceride content of sunflower oil.

Table 2 reports the effects of varying the adsorbed particle size on the average coalescence times observed after a 2-min droplet aging time. Because of the much higher turbidity of the 902-nm particle dispersions, experiments were conducted only at a dispersion concentration of 5.3×10^{-4} wt %. At higher concentrations, the dispersions were not sufficiently optically transparent, and thus, coalescence events could not be observed. At this relatively low concentration, the adsorbed particles at the droplet interface were not close-packed. Indeed, based on the total interfacial area of the two droplets plus the top planar oil/water interface of the beaker and assuming a packing efficiency of 0.9 in accordance with hexagonal close packing,[43] it can be calculated that the maximum coverage fraction at this concentration was only 0.4 (see Table S1, Supporting Information). However, in contrast to the bare oil/water interfaces, coalescence did occur when the latex particles were adsorbed at the surface of the droplets. The near-zero zeta potential of these adsorbed latex particles[30] provides little or no electrostatic barrier to droplet coalescence in aqueous solution. In addition, the repulsive capillary pressure ($\sim 1/r$) across the near-planar interfaces when the 2-mm oil droplets come into contact is relatively insignificant compared to that stabilizing the 50-μm droplets in the bulk emulsion against coalescence for several months.[24]

Table 2. Effects of Oil Type, Particle Size, Concentration, and Mixed Particle Dispersions on the Coalescence Time of Two Interacting *n*-Dodecane or Sunflower Oil Droplets Grown and Aged for 2 min in the Presence of Aqueous $PGMA_{50}$–PS Particle Dispersions

oil type	$PGMA_{50}$–PS particle diameter (nm)	particle concentration (wt %)	coalescence time (s)
n-dodecane	902	5.3×10^{-4} [a]	77 ± 55 (8 s–2.7 min)[b]
n-dodecane	135	7.8×10^{-5} [a]	0.9 ± 0.2
n-dodecane	135	1.9×10^{-3}	0.6 ± 0.2
n-dodecane	135 + 902[c]	7.8×10^{-5} + 5.3×10^{-4}	1.0 ± 0.1
sunflower oil	902	5.3×10^{-4} [a]	148 (3 s–15 min)[b]
sunflower oil	135	7.8×10^{-5} [a]	23.2 ± 6.7
sunflower oil	135	1.9×10^{-3}	19.0 ± 5.4
sunflower oil	135 + 902[c]	7.8×10^{-5} + 5.3×10^{-4}	20.3 ± 9.6

[a]Particle concentrations correspond to a total projected particle surface area (cross-sectional area of one particle × number of particles) of 4.1×10^{-4} m^2 for both particle sizes. [b]With 53% of the coalescence times occurring within 100 s (see Figure 2) [c]Droplets were grown in a binary aqueous dispersion of both particles.

The data in Table 2 indicate that, on average, sunflower oil droplets took a longer time to coalesce irrespective of which particles were present at the interface. This is thought to be due to two factors. First, the lower interfacial tension of the sunflower oil/water interface should result in a flatter contact zone between the two droplets and, hence, a larger area subject to film drainage immediately prior to coalescence. Second, the increased viscosity of the sunflower oil is expected to hinder particle rearrangements on the interface during the thin-film drainage process and reduce the possibility of thin-film rupture where defects exist in the particle packing.

Interestingly, when the 902-nm particles were adsorbed at the interface, the spread in the coalescence times for both oil types was large, with a few longer coalescence times positively skewing the data in both cases (see Figure 2). These data suggest two different modes of contact between impinging oil

dx.doi.org/10.1021/la3025765 | *Langmuir* 2012, 28, 16501–16511

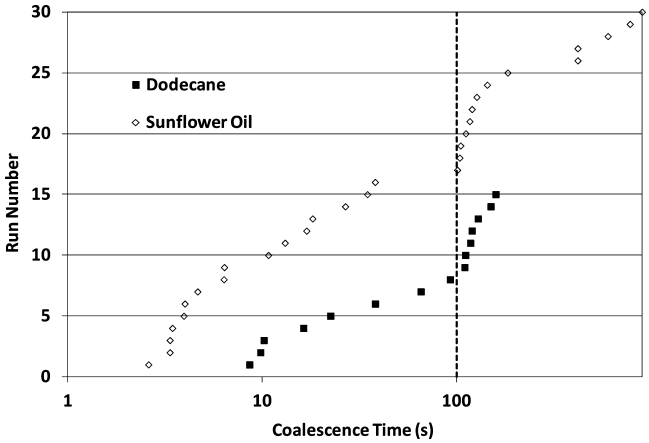

Figure 2. Positively skewed cumulant distributions for coalescence times for droplets of sunflower oil and *n*-dodecane armored with the 902-nm particles. The change in curvature at 100 s in each distribution is suggestive of two different modes of coalescence that are independent of the oil viscosity: for example, above 100 s is dominated by bilayer contact, whereas below 100 s is dominated by monolayer contact.

droplets during thin-film drainage, leading to two distinct coalescence modes and thus characteristic times. When the two latex-adsorbed droplets are brought into contact the drainage of the thin film between the droplets is expected to facilitate the rearrangement of the latex particles at the interface and effectively to close-packed particles in the contact zone. The droplets could then be bridged by either a bilayer or monolayer of particles (see Figure 3), with the former being most likely in the first instance.[44] As the aqueous film drains, any packing defects in the opposing particle monolayers could result in either a jump to the bridging monolayer scenario or direct droplet coalescence when oil from the two droplets is able to come into contact. This drainage model indicates the possibility of two different droplet separation distances, D (see Figure 3). Because of the much thicker aqueous film, a bilayer of hexagonally close-packed particles should lead to significantly more stable droplets and, hence, produce the relatively long coalescence times that skew the data sets. In contrast, more rapid coalescence should be observed when only a bridging hexagonally close-packed monolayer of particles separates the droplets.[45,46] The presence of the adsorbed latex particles creates a physical barrier to coalescence but does not prevent it.

Table 2 also lists the mean coalescence times observed for oil droplets coated with 135-nm $PGMA_{50}$–PS particles at two different latex concentrations. The lower concentration was chosen to match the interfacial coverage obtained with the larger latex particles, which was limited in practice by the significant turbidity resulting from the larger particles. At this concentration, it is likely that the adsorbed latex particles were not close-packed on the surface of the droplets. The higher concentration was estimated (see Table S1, Supporting Information) to correspond to a maximum of 11% of the particles in solution being adsorbed at the oil/water interface, that is, an excess of nonadsorbed particles was present. However, for both *n*-dodecane and sunflower oil, there appeared to be little effect of latex concentration on the droplet coalescence times. This indicates that the packing of the smaller latex particles in the contact zone was equivalent for both bulk solution concentrations, supporting the notion that the packing fraction of particles in this region was enhanced

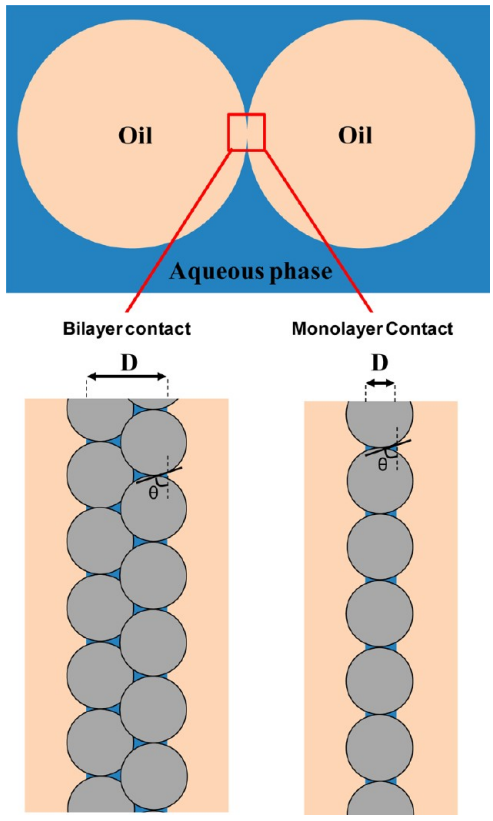

Figure 3. Schematic representation of the estimated oil/water/oil minimum separation upon contact of two oil droplets coated with hexagonally close-packed monolayers of latex particles. The aqueous film thickness D was estimated to be 145 and 35 nm, respectively, for the bilayer and monolayer films formed by the small 135-nm latex particles. The aqueous film thickness was estimated to be D = 970 nm and D = 230 nm, respectively, for the bilayer and monolayer films for the large 902-nm latex particles.[45,46].

during thin-film drainage. On average, adsorption of the 135-nm latex onto either *n*-dodecane or sunflower oil droplets led to reduced coalescence times compared to the corresponding interfaces coated with the 902-nm latex. This is attributed to the shorter separation distance between the oil phases when the two giant Pickering emulsion droplets were brought into contact (See Figure 3). The skewed data sets were recorded only for the larger latex, which suggests that there was insufficient temporal resolution to distinguish between these two coalescence modes within the short coalescence times for the droplets coated with the smaller latex.

Sequences of images showing the coalescence of two *n*-dodecane and sunflower oil droplets in the presence of the higher concentration of 135-nm latex particles are shown in Figures 4 and 5 (and Supporting Information videos 1 and 2), respectively. Comparison of image 1 of these two figures does indeed indicate a larger contact zone for the sunflower oil droplets prior to coalescence. Further comparison of these two sets of images highlights the viscosity difference between the two oils, with the postrupture motion substantially damped in the case of the higher-viscosity sunflower oil. The corresponding coalescence dynamics after a frame-by-frame analysis of the video footage appears in Figure 6A. The projected area oscillations resulting from coalescence were highly damped in the case of sunflower oil when compared to the longer oscillation of the coalesced *n*-dodecane droplet; such behavior

dx.doi.org/10.1021/la3025765 | *Langmuir* 2012, 28, 16501−16511

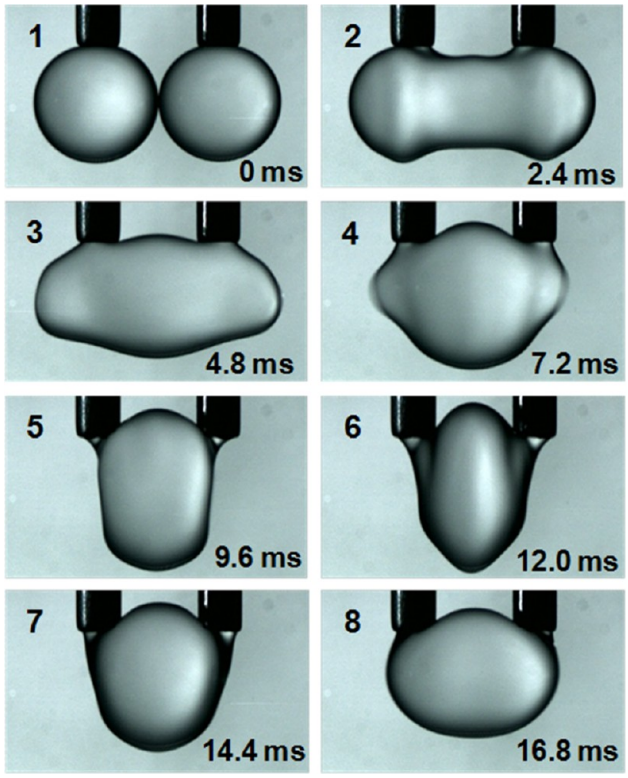

Figure 4. Sequence of images (every fifth frame) recorded for coalescing *n*-dodecane droplets in the presence of a 1.9×10^{-3} wt % aqueous dispersion of 135-nm $PGMA_{50}$–PS latex particles. The outer diameter of the needles was 0.71 mm, which provides an appropriate scale bar.

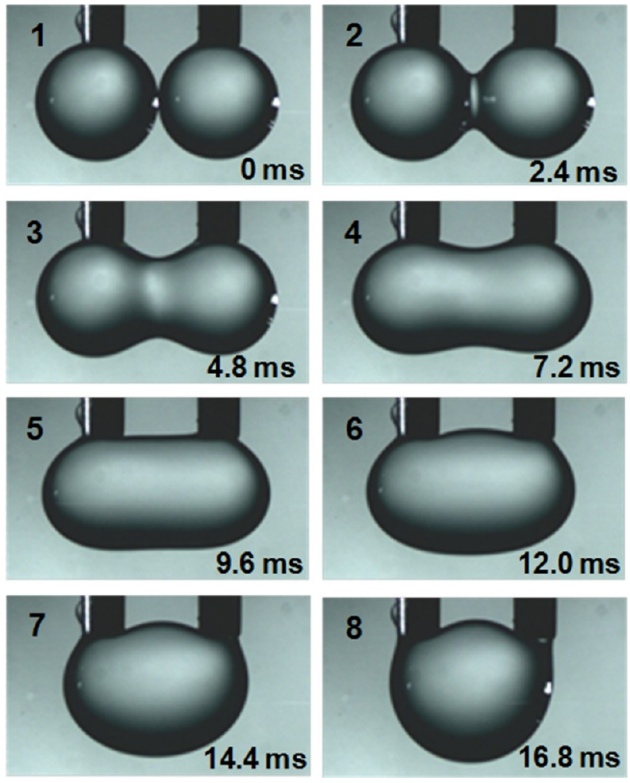

Figure 5. Sequence of images (every fifth frame) recorded for coalescing sunflower oil droplets in the presence of a 1.9×10^{-3} wt % aqueous dispersion of 135-nm $PGMA_{50}$–PS latex particles. The outer diameter of the needles was 0.71 mm, which provides an appropriate scale bar.

was also observed for the bare droplet experiments (Figure S1, Supporting Information). When these oscillatory data were fitted to a damped simple harmonic oscillator, the damping-rate coefficients were found to be 0.0674 and 0.0424 $m \cdot s^{-1}$ for the sunflower oil and *n*-dodecane Pickering droplets, respectively. The damping coefficient for sunflower oil was found to be essentially the same in the presence and absence of particles (0.0674 versus 0.0671 $m \cdot s^{-1}$). However, the corresponding coefficient for *n*-dodecane was significantly larger when the particles were present. This is direct evidence for adsorption of the latexes at the *n*-dodecane/water interface, which, in turn, leads to greater damping of the coalescence oscillation. The even stronger damping of the coalescing sunflower oil/water interfaces masks any impact of adsorbed particles, as the damping is dominated by the significantly higher viscosity of the sunflower oil.

The postrupture oscillations for *n*-dodecane droplets coated with the large and small latex particles are shown in Figure 6B. The direct superposition of the two curves indicates that there is no difference in the energy of the coalescence process once the thin aqueous film has ruptured. It is emphasized here that the bulk concentrations in these experiments were below that required for close-packing in the case of the large latex, but approximately 10 times greater than that required for close-packing of the smaller latex (see Table S1, Supporting Information). The data in Figure 6B thus imply that the mere presence of particles at the interface is more important than their packing in affecting the postrupture dynamics of the interface.

Also reported in Table 2 are experiments where the smaller and larger latexes were added to the sample beaker at the same time and oil droplets were grown in the presence of both types of particles. Initially, a one-off experiment was performed whereby the 902-nm particles were added to a dispersion of 135-nm particles in which two droplets had already been grown and aged for 2 min. For both *n*-dodecane and sunflower oil, there was no change in coalescence time when compared to that of the small particles alone. This suggests that the presence of the 902-nm latex particles in the contact zone was not sufficient to greatly alter the coalescence event. That is, the narrower thin film formed in the presence of the 135-nm latex dominated the interaction. Subsequently, a series of oil droplets were grown in the binary aqueous dispersions containing both latexes, at concentrations of approximately equivalent projected interfacial area. Again, the coalescence times were the same within error for both oils as those achieved with the small particles alone. This suggests that the smaller particles preferentially adsorb at the oil/water interface or at least are present in sufficient concentration to dominate the interaction in the contact zone. This is consistent with the much higher diffusion coefficient of the 135-nm particles, which thus reach the surface of the oil droplets more quickly. Once adsorbed, they are not displaced from this interface by the larger particles.

Pendant Colloidosome Interactions. The possibility of creating pendant colloidosomes was investigated by adding PPG-TDI cross-linker to sunflower oil. This cross-linker has previously been used in conjunction with $PGMA_{50}$–PS particles to prepare covalently cross-linked colloidosomes through both conventional homogenization[24,25] and stirred-

dx.doi.org/10.1021/la3025765 | *Langmuir* 2012, 28, 16501–16511

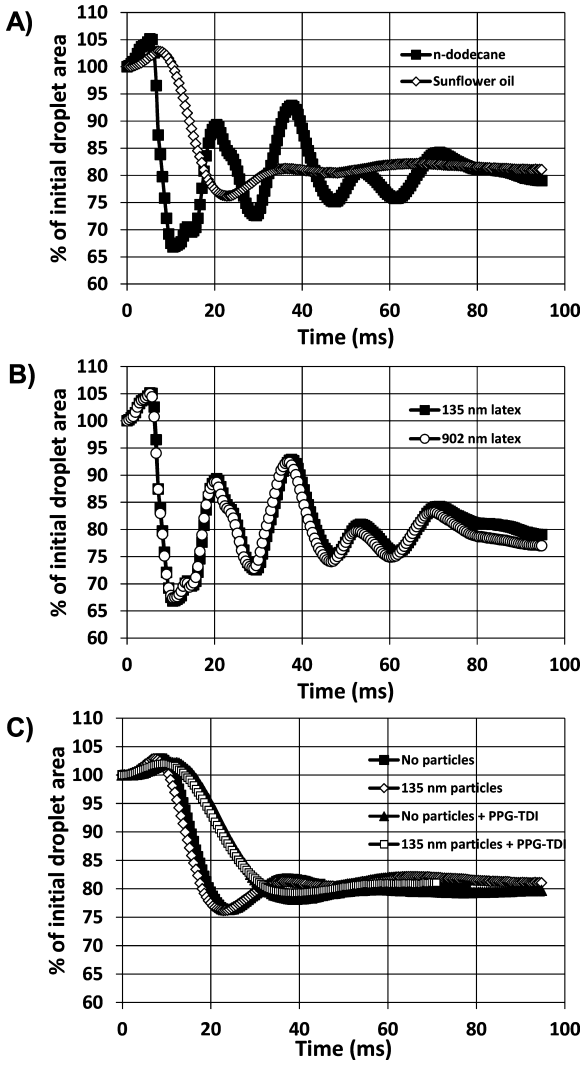

Figure 6. Comparison of the coalescence dynamics of (A) two *n*-dodecane and sunflower oil droplets prepared in the presence of a 1.9 × 10^{-3} wt % aqueous dispersion of 135-nm $PGMA_{50}$–PS latex particles, (B) two *n*-dodecane droplets in the presence of either 135- or 902-nm $PGMA_{50}$–PS latex particles, and (C) sunflower oil droplets in both the presence and absence of 135-nm $PGMA_{50}$–PS latex particles and 1 mg/mL PPG-TDI cross-linker. Note that 0.1 M KCl was used to observe coalescence of the bare oil droplets in panel A.

cell membrane emulsification.[47] Previous studies on both the small and large latexes have shown that a reaction time of approximately 20 min is required to cross-link neighboring $PGMA_{50}$–PS particles to form colloidosomes that are sufficiently robust to survive washing with excess ethanol. Therefore, cross-linking times of 2–10 and ≥20 min were investigated; see Table 3. It should be noted that the pairs of droplets were not placed in contact during the period allowed for cross-linking. The mean coalescence times observed when the PPG-TDI-loaded droplets were aged for between 2 and 10 min were approximately twice those observed when no cross-linker was present. Although this suggests that cross-linking does occur, droplets that are insufficiently cross-linked cannot withstand coalescence, which is consistent with the earlier emulsion work. The greater variation in the coalescence times observed for oil droplets of intermediate age that contain PPG-TDI is attributed to the extent of the cross-linking reaction, which is expected to depend on the nearest-neighbor distance

Table 3. Effect of Cross-Linking Time on the Coalescence Time of Two 2-mm Sunflower Oil Droplets in the Presence of a 1.9 × 10^{-3} wt % Aqueous Solution of 135-nm $PGMA_{50}$–PS Particles

cross-linker concentration (mg/mL)	cross-linking time (min)	coalescence time (s)
0	0	19 ± 5
1	2–10	43 ± 34
1	>20	no coalescence

between adsorbed particles (see Figure S2, Supporting Information). That is, packing defects are expected to result in less efficient cross-linking and thus shorter coalescence times.

Droplet aging of 20 min or more prevented coalescence in the presence of excess 135-nm $PGMA_{50}$–PS particles. This suggests that the cross-linking of close-packed adsorbed particles to form giant colloidosomes occurs on the same time scale as reported previously for 50–100-μm Pickering emulsion droplets.[25] This can be explained by considering the interparticle separation at the oil/water interface. This is estimated to be equal to $(d - d_c)$, where d is the mean particle diameter and d_c is the chord length at the interface (see Figure S2, Supporting Information). The oil-soluble PPG-TDI will react with the hydroxyl groups of the PGMA stabilizer chains located in the oil phase, thereby cross-linking neighboring particles that are sufficiently close together. Based on a contact angle of approximately 75°,[42] the interfacial interparticle separation is estimated to be 4.6 nm for the smaller latex. The length of the PPG-TDI molecule is estimated to be at most 15 nm, which suggests that the cross-linking reaction can be readily achieved for the small latex when adsorbed in a close-packed arrangement. For the larger latex, for which optical observations were limited to lower concentrations, coalescence was always observed when PPG-TDI was present in the oil phase. This is strong evidence that, at this concentration, these larger particles were not close-packed at the oil/water interface and that the presence of the surface-active cross-linker alone cannot prevent coalescence. It should be noted that earlier work in which cross-linked colloidosomes were prepared in bulk aqueous solution using the larger latex particles utilized a much higher concentration of particles.[24]

Similar giant colloidosomes were not formed at the *n*-dodecane/water interface even in the presence of an excess of the smaller latex, despite their formation from the Pickering emulsions prepared by homogenization.[24,25] This puzzling result is attributed to the poorer solubility of PPG-TDI in *n*-dodecane. The more globular form of PPG-TDI in *n*-dodecane presumably precludes this reagent from bridging the interfacial interparticle distance efficiently in the absence of applied shear, even in the case of a close-packed adsorbed layer of the 135-nm latex.[48] That PPG-TDI successfully cross-linked the Pickering emulsions formed under high shear using these latexes suggests that homogenization might coat the particles with the cross-linking agent, facilitating more efficient reactivity than that occurring under the diffusion-limited conditions utilized for the giant pendant droplets investigated in the present study.

The oscillatory behavior of the coalescence events of giant sunflower oil droplets prepared with and without added PPG-TDI and in the presence and absence of particles is shown in Figure 6C. The significant difference observed here compared to that observed for the pure oil/water interface is attributed to the presence of PPG-TDI at the solution/water interface. The

dx.doi.org/10.1021/la3025765 | *Langmuir* 2012, 28, 16501–16511

pendant drop method for determining the interfacial tension utilized here relies on fitting a shape profile to an image of a single droplet in order to calculate its volume and surface area. When particles of high density are present at the droplet surface, some shape distortion is possible because of buildup of particles at the bottom of the droplet.[31] This limitation is not apparent in the measurements performed here, as the density of the polymer latex was close to that of both fluid phases. In fact, no impact of the adsorbed 135-nm latex particles on the interfacial tension could be detected in either the absence or presence of the highly surface-active PPG-TDI cross-linker (see Table 1). This indicates that (i) the presence of adsorbed PPG-TDI molecules at the oil/water interface dominates the interfacial tension and (ii) the enhanced stability of the giant colloidosomes is due to the steric barrier to coalescence conferred by cross-linking the latex rather than any reduction in the interfacial energy of the system. However, the increase in the damping coefficient due to PPG-TDI that is evident in Figure 6C cannot be explained by the interfacial tension alone, as this would be expected to reduce the damping coefficient for the coalescing droplet (as observed for the pure oils in Figure 6A), rather than increase it.[49] In addition, because there is no increase in the bulk viscosity upon the addition of PPG-TDI to sunflower oil, an alternative explanation was sought for the increase in the damping coefficient seen in Figure 6C.

The dynamic interfacial rheological properties of sunflower oil droplets in aqueous dispersions containing an excess of the 135-nm latex, with and without PPG-TDI cross-linker, are shown in Figure 7. The droplets were aged for up to 2 h prior to the applied volume oscillations. The data show two distinct behaviors depending on whether PPG-TDI was present, in accordance with the data shown in Figure 6C. The interfacial elasticity and dilational viscosity shown in parts A and B, respectively, of Figure 7 were calculated from the response in interfacial tension and droplet area to the applied sinusoidal change in droplet volume. The elasticity derives from the magnitude of the response, whereas the dilational viscosity is derived from the phase lag and can be related to the rate of exchange of matter between the interface and the bulk.[50] In the absence of cross-linker, no change was observed in either interfacial elasticity or dilational viscosity with droplet aging time. However, when the cross-linker was present in the oil droplet, both interfacial elasticity and dilational viscosity decreased markedly for short aging times and further decreased significantly as the droplet is aged for at least 20 min. A similar reduction in these two interfacial parameters was recorded for PPG-TDI-dosed oil droplets aged for short times in the absence of latex particles. This suggests that the change in postrupture dynamics observed in Figure 6C for the coalescence of droplets aged for ≤10 min is due to the reduction in these interfacial rheological parameters and that the presence of the cross-linker at the interface dominates these behaviors. The reduced interfacial elasticity implies that the interfacial tension changes less as the droplet surface area is oscillated, whereas the reduced dilational viscosity suggests that the interface responds faster to changes in volume. Both factors suggest that the droplet should be more robust and more tolerant to deformation, as evidenced by the stronger damping shown in Figure 6C. Ata et al. previously hypothesized that the greater damping observed in the motion of coalescing kerosene droplets correlates with a reduction in interfacial elasticity,[34] but in the present study, this correlation was directly observed.

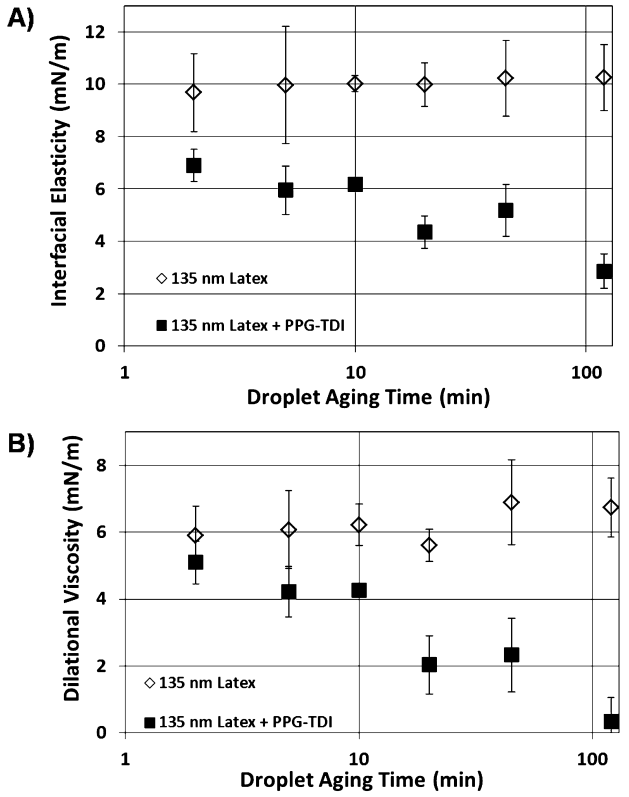

Figure 7. (A) Interfacial elasticity and (B) dilational viscosity as logarithmic functions of aging time observed for pendant sunflower oil droplets in the presence of 1.3×10^{-3} wt % 135-nm particles and PPG-TDI cross-linker. Pendant drops with a volume of 10 μL were left to age before the application of a sinusoidal ± 1 μL volume change with a 5-s period.

When the droplets were aged independently for more than 20 min in the presence of PPG-TDI, coalescence was never observed when the droplets were moved into contact. Instead, they remained completely stable for periods of several hours, after which they could be moved apart again. This is in good agreement with the minimum cross-linking time estimated for bulk Pickering emulsions,[25] as well as the further reduction in interfacial elasticity and dilational rheology for extended droplet aging times in Figure 7. Figure 8 shows a sequence of images recorded for two giant colloidosomes after these droplets had been aged independently for 20 min. The droplets were brought into contact and left for a further 25 min before the capillaries were moved back to their original starting positions. A distinct neck connecting the two pendant colloidosomes can clearly be observed in images 2 and 3. This adhesion could be evidence for the onset of intercolloidosome fusion, a phenomenon that was not observed for the smaller colloidosomes prepared in earlier work.[24] It is worth emphasizing that the droplet diameter in the current work was significantly greater than that obtained for Pickering emulsions prepared by homogenization (2 mm versus 50 μm). This greater size leads to a considerably larger and flatter contact zone between the oil droplets, which could explain the intercolloidosome adhesion observed in this case. Usually, a coalescence event occurs as water drains out of the thin film between the oil droplets in contact. In the case of the cross-linked pendant colloidosomes, this drainage can still occur, but coalescence is prevented as the particles are locked in position. It might be that, after a sufficiently long contact time, the oil

dx.doi.org/10.1021/la3025765 | Langmuir 2012, 28, 16501−16511

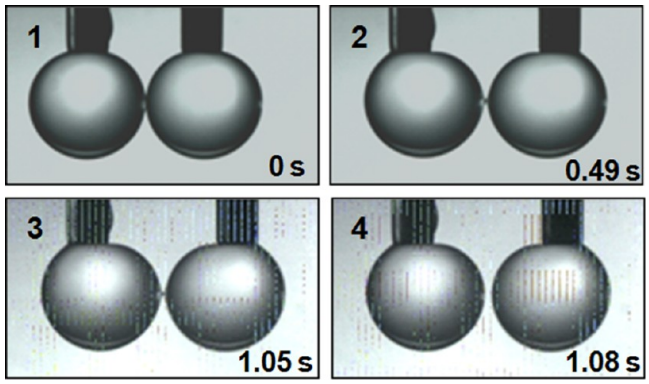

Figure 8. Sequence of images of two pendant colloidosomes upon moving apart. The colloidosomes were formed when sunflower oil droplets containing PPG-TDI cross-linker were exposed to a 1.9×10^{-3} wt % aqueous dispersion of 135-nm $PGMA_{50}$–PS latex particles. The droplets were aged in isolation for 20 min before being moved into contact. After a further 25 min in contact (image 1), the droplets were moved apart again (images 2–4). A neck connecting the two pendant colloidosomes can be clearly observed in images 2 and 3.

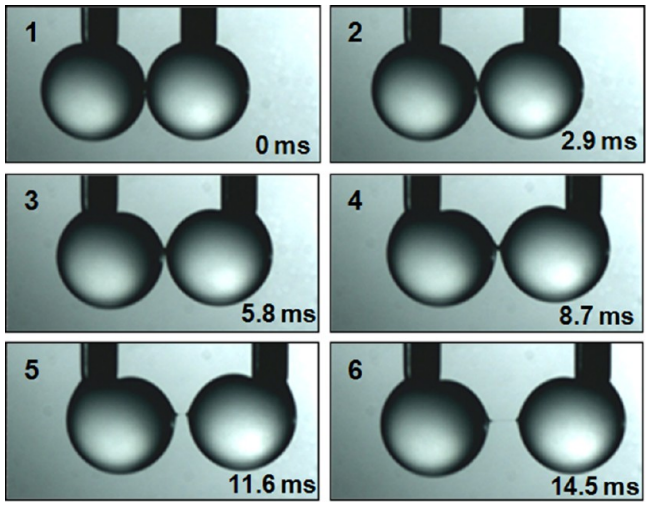

Figure 9. Still images taken from the asymmetric droplet experiment showing two droplets grown in the presence of a 1.9×10^{-3} wt % aqueous dispersion of 135-nm $PGMA_{50}$–PS particles being moved apart. The left-hand droplet contained pure sunflower oil, and the right-hand droplet contained PPG-TDI cross-linker in sunflower oil. The droplets were aged in isolation for 20 min before being moved into contact. They were left in contact for 2 h and then moved apart.

(and thus cross-linker) could penetrate this contact zone and cross-link the latex particles on the surface of the adjacent droplets. In principle, this could lead to the neck formation observed in Figure 8. However, the neck was readily broken upon moving the capillaries apart, and the symmetry of the pendant colloidosomes in image 4 indicates that the two are of similar structural integrity.

Asymmetric Interactions. A series of experiments with asymmetric droplets was also conducted to examine the effect of having the cross-linker confined to just one of the pendant droplets. The same trend in droplet stability was observed as when the cross-linker was present in both oil droplets: After 20 min of aging, the droplet pairs that were moved into contact never underwent coalescence. This shows that only one of the oil droplets needs to be cross-linked to prevent coalescence. Figure 9 (and Supporting Information video 3) shows a series of still images recorded when two sunflower oil droplets that had been left in contact for 2 h were moved apart. The left-hand Pickering droplet initially contained pure sunflower oil, whereas the right-hand colloidosome droplet contained PPG-TDI cross-linker. First, the asymmetric droplets were sufficiently stable to survive being left in contact for 2 h. Upon being separated (at a rate of 2.38 mm/s), the droplets were connected by a bridge (images 2 and 3) as observed for the symmetrical colloidosomes shown in Figure 8. However, image 4 highlights the greater strength of this interaction, as the two droplets were held together sufficiently strongly to result in substantial asymmetry in their positions on the needles. In addition, the neck between the two droplets stretched to form a long connecting filament that did not break, despite being elongated by several millimeters (images 5 and 6). This filament was extended to the maximum possible separation of the capillaries (3.15 mm) without breaking. In addition, upon expanding image 6, we estimated this filament to be on the order of tens of micrometers in thickness. The character and behavior of the filament provides good evidence that the cross-linker diffused across the contacting particle bilayer while the droplets were in contact for 2 h, ultimately cross-linking the left-hand droplet to form a second colloidosome. This suggests that most of the water readily drained from the thin film, as the cross-linker is not water-soluble. In the case of the un-cross-linked Pickering droplets (Figures 4 and 5), this drainage of water from the thin film separating the drops resulted in the observed coalescence. It is also highly likely that the filament in Figure 9 contained cross-linked particles, but that the neck arising from the shorter contact time of 25 min (shown in Figure 8) did not.

■ CONCLUSIONS

In summary, we have investigated the interactions of bare Pickering-type and colloidosome-stabilized oil droplets. We found that bare oil droplets exhibit surprising stability in the absence of adsorbed latex, which is consistent with the recent literature. In the presence of latex particles, the droplets always coalesced. The characteristic coalescence times were generally found to be shorter on switching from the 902-nm latex to the 135-nm latex and also when changing the oil phase from *n*-dodecane to sunflower oil. The particle size effect is consistent with a larger oil droplet separation distance and thus aqueous thin-film thickness. Sunflower oil has a lower interfacial tension and a higher viscosity than *n*-dodecane, both of which contribute to the longer coalescence times observed for the former oil. The observed coalescence times also provide evidence of two modes of droplet contact, which is consistent with bilayer and monolayer particle bridging between oil droplets in the contact zone.

The presence of latex particles increases the damping coefficient at the *n*-dodecane/water interface, which confirms that particle adsorption has occurred. In contrast, the damping coefficient of the sunflower oil/water interface is dominated by the much higher viscosity of this oil. When both latexes are present together in solution, the presence of the smaller particles in the contact zone dominates the coalescence event.

Addition of an oil-soluble polymeric cross-linker (PPG-TDI) to the sunflower oil phase prevented droplet coalescence in the case of the 135-nm latex over a time scale of at least 20 min. At shorter aging times, the cross-linker markedly reduced both the interfacial elasticity and the dilational rheology, yielding

dx.doi.org/10.1021/la3025765 | *Langmuir* 2012, 28, 16501–16511

droplets that were more tolerant to deformation; this behavior was correlated to stronger damping in the postcoalescence dynamics. Even further reduction in these two interfacial rheological parameters was observed for droplets aged beyond 20 min. Thus, the cross-linking reaction in the giant colloidosomes was consistent with the rate of cross-linking observed in previous experiments on emulsification by homogenization. Perhaps surprisingly, this cross-linking chemistry did not prevent coalescence when *n*-dodecane was used as the oil. This result is attributed to the reduced solubility of PPG-TDI in this phase. Moreover, this result indicates that the relatively high shear required for emulsion homogenization[24] is capable of mixing PPG-TDI and enabling cross-linking to occur more efficiently than in the case of the diffusion-limited giant colloidosome system detailed here.

Finally, asymmetric experiments demonstrated that only one droplet needs to contain the PPG-TDI cross-linker for coalescence to be completely prevented. Interestingly, after long contact times (~2 h), a filament was observed connecting the two droplets upon their separation. This suggests that the cross-linker diffuses into the neighboring droplet during contact, indicating that interdroplet mass transport can occur.

■ ASSOCIATED CONTENT

Supporting Information

Figures showing (1) the coalescence dynamics of uncoated pairs of oil droplets in aqueous solution and (2) the distance that the cross-linking molecule must stretch between particles at the oil/water interface. Table listing example calculations of maximum area occupied by particles at the oil/water interface. Representative videos of two pendant droplets recorded in 1.9×10^{-3} wt % 135-nm latex dispersions for (1) *n*-dodecane droplets and (2) sunflower oil droplets. Video 3 shows the formation of the filament observed in the asymmetric cross-linker experiment. (The videos contain every 25th frame of the original recordings at 2100 frames/s.) This material is available free of charge via the Internet at http://pubs.acs.org.

■ AUTHOR INFORMATION

Corresponding Author

*E-mail: erica.wanless@newcastle.edu.au.

Notes

The authors declare no competing financial interest.

■ ACKNOWLEDGMENTS

E.J.W. and S.A. thank the Australian Research Council for DP120102305. K.L.T. acknowledges the EPSRC/The University of Sheffield for a University Doctoral Prize Fellowship. G. Bournival is thanked for providing training on the coalescence rig. J. Smith is thanked for the bulk viscosity measurement. P. Ireland is thanked for suggestions concerning coalescence statistics. B. Cheesman is thanked for checking the purity of the sunflower oil by NMR spectroscopy. The reviewers are thanked for their insight and suggestions, and S.-Y. Tan is thanked for help with the manuscript revisions.

■ REFERENCES

(1) Pickering, S. U. Emulsions. *J. Chem. Soc.* **1907**, *91*, 2001−2021.
(2) Binks, B. P. Particles as surfactants—Similarities and differences. *Curr. Opin. Colloid Interface Sci.* **2002**, *7* (1−2), 21−41.
(3) Binks, B. P.; Whitby, C. P. Silica Particle-Stabilized Emulsions of Silicone Oil and Water: Aspects of Emulsification. *Langmuir* **2004**, *20* (4), 1130−1137.
(4) Cui, Y.; Threlfall, M.; van Duijneveldt, J. S. Optimizing organoclay stabilized Pickering emulsions. *J. Colloid Interface Sci.* **2011**, *356* (2), 665−671.
(5) Amalvy, J. I.; Unali, G. F.; Li, Y.; Granger-Bevan, S.; Armes, S. P.; Binks, B. P.; Rodrigues, J. A.; Whitby, C. P. Synthesis of sterically stabilized polystyrene latex particles using cationic block copolymers and macromonomers and their application as stimulus-responsive particulate emulsifiers for oil-in-water emulsions. *Langmuir* **2004**, *20* (11), 4345−4354.
(6) Amalvy, J. I.; Armes, S. P.; Binks, B. P.; Rodrigues, J. A.; Unali, G. F. Use of sterically-stabilised polystyrene latex particles as a pH-responsive particulate emulsifier to prepare surfactant-free oil-in-water emulsions. *Chem. Commun.* **2003**, *15*, 1826−1827.
(7) Binks, B. P.; Murakami, R.; Armes, S. P.; Fujii, S. Temperature-induced inversion of nanoparticle-stabilized emulsions. *Angew. Chem., Int. Ed.* **2005**, *44* (30), 4795−4798.
(8) Fujii, S.; Armes, S. P.; Binks, B. P.; Murakami, R. Stimulus-responsive particulate emulsifiers based on lightly cross-linked poly(4-vinylpyridine)-silica nanocomposite microgels. *Langmuir* **2006**, *22* (16), 6818−6825.
(9) Binks, B. P.; Horozov, T. S. Aqueous foams stabilized solely by silica nanoparticles. *Angew. Chem., Int. Ed.* **2005**, *44* (24), 3722−3725.
(10) Binks, B. P.; Murakami, R. Phase inversion of particle-stabilized materials from foams to dry water. *Nat. Mater.* **2006**, *5* (11), 865−869.
(11) Fujii, S.; Randall, D. P.; Armes, S. P. Synthesis of Polystyrene/Poly[2-(Dimethylamino)ethyl Methacrylate-*stat*-Ethylene Glycol Dimethacrylate] Core−Shell Latex Particles by Seeded Emulsion Polymerization and Their Application as Stimulus-Responsive Particulate Emulsifiers for Oil-in-Water Emulsions. *Langmuir* **2004**, *20* (26), 11329−11335.
(12) Binks, B. P.; Lumsdon, S. O. Pickering emulsions stabilized by monodisperse latex particles: Effects of particle size. *Langmuir* **2001**, *17* (15), 4540−4547.
(13) Dinsmore, A. D.; Hsu, M. F.; Nikolaides, M. G.; Marquez, M.; Bausch, A. R.; Weitz, D. A. Colloidosomes: Selectively permeable capsules composed of colloidal particles. *Science* **2002**, *298* (5595), 1006−1009.
(14) Yow, H. N.; Routh, A. F. Release Profiles of Encapsulated Actives from Colloidosomes Sintered for Various Durations. *Langmuir* **2009**, *25* (1), 159−166.
(15) Laib, S.; Routh, A. F. Fabrication of colloidosomes at low temperature for the encapsulation of thermally sensitive compounds. *J. Colloid Interface Sci.* **2008**, *317* (1), 121−129.
(16) Paunov, V. N.; Noble, P. F.; Cayre, O. J.; Alargova, R. G.; Velev, O. D. Fabrication off novel types of colloidosome microcapsules for drug delivery applications. *Nanoscale Mater. Sci. Biol. Med.* **2005**, *845*, 279−283.
(17) Noble, P. F.; Cayre, O. J.; Alargova, R. G.; Velev, O. D.; Paunov, V. N. Fabrication of "hairy" colloidosomes with shells of polymeric microrods. *J. Am. Chem. Soc.* **2004**, *126* (26), 8092−8093.
(18) Gordon, V. D.; Xi, C.; Hutchinson, J. W.; Bausch, A. R.; Marquez, M.; Weitz, D. A. Self-assembled polymer membrane capsules inflated by osmotic pressure. *J. Am. Chem. Soc.* **2004**, *126* (43), 14117−14122.
(19) Caruso, F.; Caruso, R. A.; Möhwald, H. Nanoengineering of Inorganic and Hybrid Hollow Spheres by Colloidal Templating. *Science* **1998**, *282* (5391), 1111−1114.
(20) Caruso, F.; Spasova, M.; Susha, A.; Giersig, M.; Caruso, R. A. Magnetic Nanocomposite Particles and Hollow Spheres Constructed by a Sequential Layering Approach. *Chem. Mater.* **2000**, *13* (1), 109−116.
(21) Yuan, Q.; Cayre, O. J.; Fujii, S.; Armes, S. P.; Williams, R. A.; Biggs, S. Responsive Core−Shell Latex Particles as Colloidosome Microcapsule Membranes. *Langmuir* **2010**, *26* (23), 18408−18414.
(22) Biggs, S.; Williams, R.; Cayre, O.; Yuan, Q. Microcapsules and methods. World Patent WO/2009/037482, 2009.
(23) Walsh, A.; Thompson, K. L.; Armes, S. P.; York, D. W. Polyamine-Functional Sterically Stabilized latexes for Covalently

Cross-linkable Colloidosomes. *Langmuir* **2010**, *26* (23), 18039−18048.
(24) Thompson, K. L.; Armes, S. P.; Howse, J. R.; Ebbens, S.; Ahmad, I.; Zaidi, J. H.; York, D. W.; Burdis, J. A. Covalently Cross-Linked Colloidosomes. *Macromolecules* **2010**, *43* (24), 10466−10474.
(25) Thompson, K. L.; Armes, S. P. From well-defined macromonomers to sterically-stabilised latexes to covalently cross-linkable colloidosomes: exerting control over multiple length scales. *Chem. Commun.* **2010**, *46* (29), 5274−6.
(26) Velev, O. D.; Furusawa, K.; Nagayama, K. Assembly of latex particles by using emulsion droplets as templates. 1. Microstructured hollow spheres. *Langmuir* **1996**, *12* (10), 2374−2384.
(27) Velev, O. D.; Furusawa, K.; Nagayama, K. Assembly of latex particles by using emulsion droplets as templates. 2. Ball-like and composite aggregates. *Langmuir* **1996**, *12* (10), 2385−2391.
(28) Velev, O. D.; Nagayama, K. Assembly of latex particles by using emulsion droplets. 3. Reverse (water in oil) system. *Langmuir* **1997**, *13* (6), 1856−1859.
(29) Ashby, N. P.; Binks, B. P.; Paunov, V. N. Formation of giant colloidosomes by transfer of pendant water drops coated with latex particles through an oil−water interface. *Phys. Chem. Chem. Phys.* **2004**, *6* (17), 4223−4225.
(30) Thompson, K. L.; Armes, S. P.; York, D. W.; Burdis, J. A. Synthesis of Sterically-Stabilized Latexes Using Well-Defined Poly(glycerol monomethacrylate) Macromonomers. *Macromolecules* **2010**, *43* (5), 2169−2177.
(31) Ata, S. Coalescence of bubbles covered by particles. *Langmuir* **2008**, *24* (12), 6085−6091.
(32) Ata, S.; Davis, E. S.; Dupin, D.; Armes, S. P.; Wanless, E. J. Direct Observation of pH-Induced Coalescence of Latex-Stabilized Bubbles Using High-Speed Video Imaging. *Langmuir* **2010**, *26* (11), 7865−7874.
(33) Dupin, D.; Howse, J. R.; Armes, S. P.; Randall, D. P. Preparation of stable foams using sterically stabilized pH-responsive latexes synthesized by emulsion polymerization. *J. Mater. Chem.* **2008**, *18* (5), 545−552.
(34) Ata, S.; Pugh, R. J.; Jameson, G. J. The influence of interfacial ageing and temperature on the coalescence of oil droplets in water. *Colloids Surf. A* **2011**, *374* (1−3), 96−101.
(35) Burnett, G. R.; Atkin, R.; Hicks, S.; Eastoe, J. Surfactant-Free "Emulsions" Generated by Freeze−Thaw. *Langmuir* **2004**, *20* (14), 5673−5678.
(36) Beattie, J. K.; Djerdjev, A. M. The pristine oil/water interface: Surfactant-free hydroxide-charged emulsions. *Angew. Chem., Int. Ed.* **2004**, *43*, 3568−3571.
(37) Roger, K.; Cabane, B. Why Are Hydrophobic/Water Interfaces Negatively Charged? *Angew. Chem., Int. Ed.* **2012**, *51* (23), 5625−5628.
(38) Marinova, K. G.; Alargova, R. G.; Denkov, N. D.; Velev, O. D.; Petsev, D. N.; Ivanov, I. B.; Borwankar, R. P. Charging of Oil−Water Interfaces Due to Spontaneous Adsorption of Hydroxyl Ions. *Langmuir* **1996**, *12* (8), 2045−2051.
(39) Tabor, R. F.; Wu, C.; Lockie, H.; Manica, R.; Chan, D. Y. C.; Grieser, F.; Dagastine, R. R. Homo- and hetero-interactions between air bubbles and oil droplets measured by atomic force microscopy. *Soft Matter* **2011**, *7* (19), 8977−8983.
(40) Liu, M.; Beattie, J. K.; Gray-Weale, A. The surface relaxation of water. *J. Phys. Chem. B* **2012**, *116*, 8981−8988.
(41) Ata, S. The detachment of particles from coalescing bubble pairs. *J. Colloid Interface Sci.* **2009**, *338* (2), 558−565.
(42) Reed, K. M.; Borovicka, J.; Horozov, T. S.; Paunov, V. N.; Thompson, K. L.; Walsh, A.; Armes, S. P. Adsorption of Sterically Stabilized Latex Particles at Liquid Surfaces: Effects of Steric Stabilizer Surface Coverage, Particle Size, and Chain Length on Particle Wettability. *Langmuir* **2012**, DOI: 10.1021/la300735u.
(43) Balmer, J. A.; Armes, S. P.; Fowler, P. W.; Tarnai, T.; Gaspar, Z.; Murray, K. A.; Williams, N. S. J. Packing Efficiency of Small Silica Particles on Large Latex Particles: A Facile Route to Colloidal Nanocomposites. *Langmuir* **2009**, *25* (9), 5339−5347.
(44) Stancik, E. J.; Kouhkan, M.; Fuller, G. G. Coalescence of Particle-Laden Fluid Interfaces. *Langmuir* **2003**, *20* (1), 90−94.
(45) Paunov, V. N. Novel Method for Determining the Three-Phase Contact Angle of Colloid Particles Adsorbed at Air−Water and Oil−Water Interfaces. *Langmuir* **2003**, *19* (19), 7970−7976.
(46) Kruglyakov, P. M.; Elaneva, S. I.; Vilkova, N. G. About mechanism of foam stabilization by solid particles. *Adv. Colloid Interface Sci.* **2011**, *165* (2), 108−116.
(47) Thompson, K. L.; Armes, S. P.; York, D. W. Preparation of Pickering Emulsions and Colloidosomes with Relatively Narrow Size Distributions by Stirred Cell Membrane Emulsification. *Langmuir* **2011**, *27*, 2357−2363.
(48) Smith, D. E.; Babcock, H. P.; Chu, S. Single-Polymer Dynamics in Steady Shear Flow. *Science* **1999**, *283* (5408), 1724−1727.
(49) Stover, R. L.; Tobias, C. W.; Denn, M. M. Bubble coalescence dynamics. *AIChE J.* **1997**, *43* (10), 2385−2392.
(50) Loglio, G.; Pandolfini, P.; Miller, R.; Makievski, A. V.; Ravera, F.; Ferrari, M.; Liggieri, L. Drop and bubble shape analysis as a tool for dilational rheological studies of interfacial layers. *Stud. Interface Sci.* **2001**, *11*, 439−483.